



## **Seeded Fault Bearing Experiments: Methodology and Data Acquisition**

**by Andrew J. Bayba, Derwin Washington, and Kwok Tom**

**ARL-TR-5575**

**June 2011**

## **NOTICES**

### **Disclaimers**

The findings in this report are not to be construed as an official Department of the Army position unless so designated by other authorized documents.

Citation of manufacturer's or trade names does not constitute an official endorsement or approval of the use thereof.

Destroy this report when it is no longer needed. Do not return it to the originator.

# **Army Research Laboratory**

Adelphi, MD 20783-1197

---

**ARL-TR-5575****June 2011**

---

## **Seeded Fault Bearing Experiments: Methodology and Data Acquisition**

**Andrew J. Bayba, Derwin Washington, and Kwok Tom**  
**Sensors and Electron Devices Directorate, ARL**

REPORT DOCUMENTATION PAGE				Form Approved OMB No. 0704-0188	
<p>Public reporting burden for this collection of information is estimated to average 1 hour per response, including the time for reviewing instructions, searching existing data sources, gathering and maintaining the data needed, and completing and reviewing the collection information. Send comments regarding this burden estimate or any other aspect of this collection of information, including suggestions for reducing the burden, to Department of Defense, Washington Headquarters Services, Directorate for Information Operations and Reports (0704-0188), 1215 Jefferson Davis Highway, Suite 1204, Arlington, VA 22202-4302. Respondents should be aware that notwithstanding any other provision of law, no person shall be subject to any penalty for failing to comply with a collection of information if it does not display a currently valid OMB control number.</p> <p><b>PLEASE DO NOT RETURN YOUR FORM TO THE ABOVE ADDRESS.</b></p>					
1. REPORT DATE (DD-MM-YYYY) June 2011		2. REPORT TYPE Final		3. DATES COVERED (From - To) October 2010 to March 2011	
4. TITLE AND SUBTITLE Seeded Fault Bearing Experiments: Methodology and Data Acquisition				5a. CONTRACT NUMBER	
				5b. GRANT NUMBER	
				5c. PROGRAM ELEMENT NUMBER	
6. AUTHOR(S) Andrew J. Bayba, Derwin Washington, and Kwok Tom				5d. PROJECT NUMBER	
				5e. TASK NUMBER	
				5f. WORK UNIT NUMBER	
7. PERFORMING ORGANIZATION NAME(S) AND ADDRESS(ES) U.S. Army Research Laboratory ATTN: RDRL-SER-E 2800 Powder Mill Road Adelphi, MD 20783-1197				8. PERFORMING ORGANIZATION REPORT NUMBER ARL-TR-5575	
9. SPONSORING/MONITORING AGENCY NAME(S) AND ADDRESS(ES)				10. SPONSOR/MONITOR'S ACRONYM(S)	
				11. SPONSOR/MONITOR'S REPORT NUMBER(S)	
12. DISTRIBUTION/AVAILABILITY STATEMENT Approved for public release; distribution unlimited.					
13. SUPPLEMENTARY NOTES					
14. ABSTRACT <p>As part of the U.S. Army Research Laboratory (ARL) Prognostics and Diagnostics (P&amp;D) Program, a series of experiments were performed to study defects in ball bearings. The P&amp;D Program objective is to develop and implement algorithms that detect and classify faults in U.S. Army systems, providing information on the state of health and predictions of remaining life. Due to the substantial use of bearings in Army assets and the significant impact of improving health assessment of bearings in operation, they were selected for a focused study, with the additional goal that any algorithms/methodologies gained by performing research on them would likely have application in other fields of health assessment. The goal of the work described here was to collect sufficient data on healthy and a variety of faulted ball bearings for evaluation of various analysis techniques.</p>					
15. SUBJECT TERMS Roller bearing analysis, bearing test rig, bearing data acquisition, seeded fault bearings					
16. SECURITY CLASSIFICATION OF:			17. LIMITATION OF ABSTRACT  UU	18. NUMBER OF PAGES  42	19a. NAME OF RESPONSIBLE PERSON Andrew J. Bayba
a. REPORT Unclassified	b. ABSTRACT Unclassified	c. THIS PAGE Unclassified			19b. TELEPHONE NUMBER (Include area code) (301) 394-0440

---

## Contents

---

<b>List of Figures</b>	<b>iv</b>
<b>List of Tables</b>	<b>v</b>
<b>1. Introduction</b>	<b>1</b>
<b>2. Experimental Setup</b>	<b>1</b>
2.1 Bearings .....	1
2.2 Test Rig .....	2
2.3 Instrumentation.....	2
2.4 Data Acquisition and Data Recording.....	3
<b>3. Experimental Procedure</b>	<b>7</b>
3.1 Overview .....	7
3.2 Rotational Frequency .....	8
3.3 Data Acquisition Software Preparation.....	8
3.4 Procedure.....	9
<b>4. Data Storage and Data Conversion</b>	<b>13</b>
<b>5. Preliminary Data Analysis and Results</b>	<b>16</b>
<b>6. Summary and Conclusions</b>	<b>22</b>
<b>Appendix. Bearing and Test Equipment Specifications</b>	<b>23</b>
<b>List of Symbols, Abbreviations, and Acronyms</b>	<b>30</b>
<b>Distribution List</b>	<b>31</b>

---

## List of Figures

---

Figure 1. Cross section of a ball bearing with nominal seeded fault locations.....	1
Figure 2. Test rig used in performing bearing experiments.....	2
Figure 3. Mounting locations and orientation of the accelerometers.....	3
Figure 4. Block diagram of data acquisition hardware. ....	4
Figure 5. eDAQ-lite data acquisition controller. ....	5
Figure 6. Accelerometer cabling and signal conditioning modules.....	6
Figure 7. Tachometer cabling focused on transition from coax to eDAQ-lite cabling.....	7
Figure 8. Test rig control panel.....	11
Figure 9. TCE software test control panel. ....	12
Figure 10. Raw time series data for a good bearing. ....	16
Figure 11. (Left) Inner race fault level 1 data and (right) inner race fault level 5 data. ....	16
Figure 12. (Left) Outer race fault level 1 data and (right) outer race fault level 5 data.....	16
Figure 13. (Left) Ball fault level 1 data and (right) ball fault level 5 data.....	17
Figure 14. Vibration RMS as a function of fault level and fault type. ....	17
Figure 15. Vibration peak to peak values as a function of fault type and fault level. ....	18
Figure 16. (Left) Good bearing envelope spectrum around BPFI and (right) fault level 1, envelope spectrum around BPFI.....	20
Figure 17. (Left) Fault level 3, envelope spectrum around BPFI and (right) fault level 5, envelope spectrum around BPFI.....	20
Figure 18. (Left) Good bearing. Envelope spectrum around BPFO and (right) fault level 1, envelope spectrum around BPFO .....	21
Figure 19. (Left) Fault level 3, envelope spectrum around BPFO and (right) fault level 5, envelope spectrum around BPFO .....	21
Figure 20. (Left) Ball fault level 1. Low end of envelope spectrum and (right) ball fault level 3, low end of envelope spectrum .....	22
Figure 21. Ball fault level 5, low end of envelope spectrum. ....	22
Figure A-1. ER16K bearing used throughout the experiments.....	23
Figure A-2. Machine fault simulator. ....	24
Figure A-3. SoMat eDAQ-lite. ....	26
Figure A-4. SoMat ICP-B-2.....	27
Figure A-5. Vibra-Metrics model 3000. ....	28

---

## List of Tables

---

Table 1. File naming and folder structure for uploaded files (no gears or load). .....	13
Table 2. File naming and folder structure for uploaded files (with gears and load).....	13
Table 3. Portion of ASCII data showing folders structure and filenames. ....	15
Table 4. Defect frequencies for these experiments. ....	19

INTENTIONALLY LEFT BLANK.

---

## 1. Introduction

---

This report documents a series of experiments that were performed to gather data on ball bearings with induced faults. The effort is part of the Prognostics and Diagnostics (P&D) Program, whose goal is to provide automated means for health assessment of Army assets in the field. The work involved the collection of vibrational data on both healthy and defective bearings when placed in service. “In service” was mimicked in the laboratory by employing the use of a Machine Fault Simulator (test rig), a specialized machine manufactured by SpectraQuest, Inc., for the purpose of examining the effects of defects in various machine components. In this study, there were three particular types of defects—ball fault, inner race fault, and outer race fault—with five levels of defect for each of the fault types.

---

## 2. Experimental Setup

---

### 2.1 Bearings

The bearings were all Rexnord ER16K ball bearings (appendix A-1). All of the bearings were new, some had defects intentionally made in them (seeded faults). There were five good bearings and 15 bearings with seeded faults. Figure 1 is a cross section of a bearing showing nominal locations of the seeded faults along with their associated components. The faulted bearings consisted of five bearings with ball faults, five bearings with inner race faults, and five bearings with outer race faults. The bearings of each fault type had five levels of damage of the specific defect. The bearings were provided as a custom order from SpectraQuest, Inc., who was also responsible for applying the faults to the bearings.

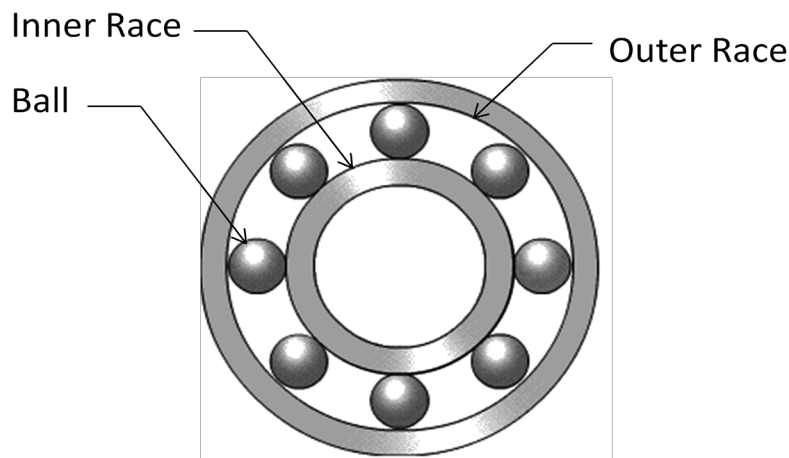


Figure 1. Cross section of a ball bearing with nominal seeded fault locations.

## 2.2 Test Rig

The bearings were placed in service, simulating real-world operation, on a test rig manufactured by SpectraQuest, figure 2 and appendix A-2. The rig is specifically designed for studying defects in machine components and is outfitted with mounting holes for accelerometers in positions of interest. As can be seen in figure 1, the rig is a complete drivetrain consisting of an electric motor; shaft with weights, pulleys, and belts; a gearbox; and a magnetic load. The shaft was loaded with two 11-lb cylindrical weights, which rotate with the shaft, and was supported by two ball bearings near the ends of the shaft. The bearing closest to the motor was the bearing under test, while the bearing further from the motor was always a known good bearing. Additionally, by removing or attaching the belts at the non-driven end of the shaft, incorporation of the gearbox and magnet load could be alternately employed (or not) in the experiment.

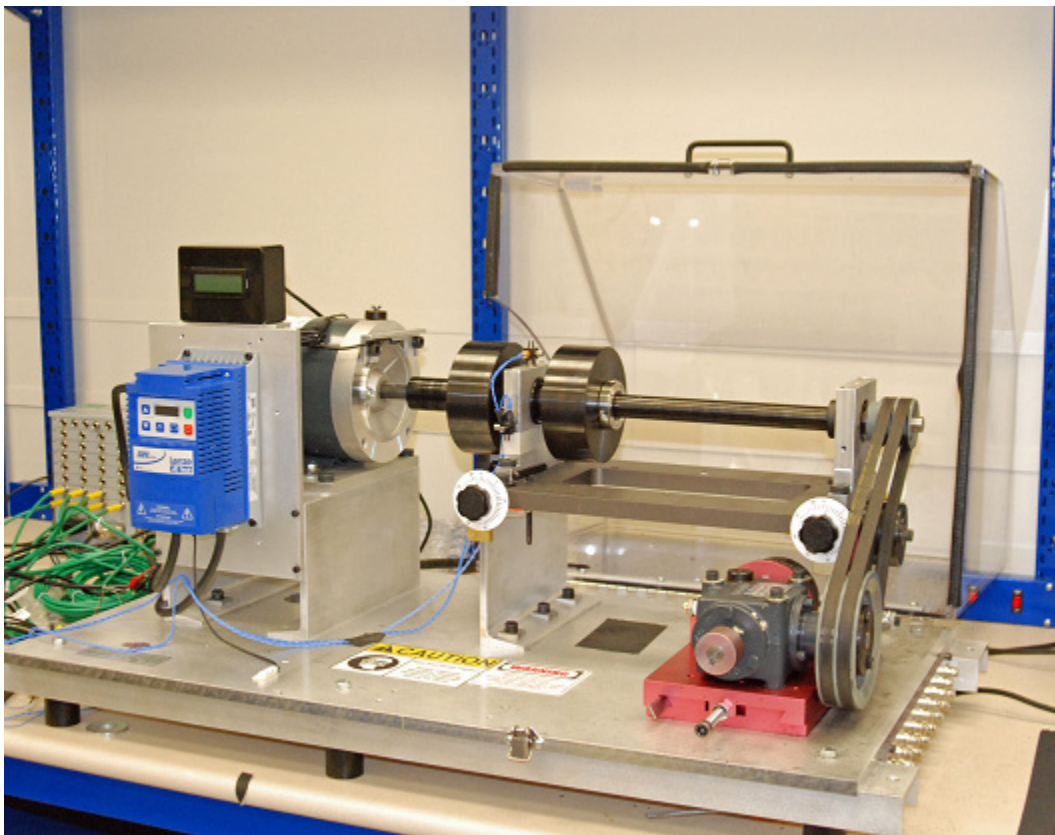


Figure 2. Test rig used in performing bearing experiments.

## 2.3 Instrumentation

### I. Tri-axial Accelerometers

The test rig was instrumented with two tri-axial accelerometers, manufactured by Vibra-Metrics, Inc (appendix A-5). The accelerometers convert mechanical vibration into analog electrical signals. These accelerometers were selected because they have the range in both amplitude and frequency to accurately measure the vibrations of interest in this study. The

maximum amplitude of the accelerometer is 500g's and it is linear at 10 mV/g from 3 Hz to 7 kHz. Both accelerometers were attached to the mounting block of the bearing under test: one directly above the bearing and one to the side of it, at 90° to the first accelerometer. The accelerometer placements and axis orientations are shown in figure 3. The x-axes of both accelerometers point in the axial direction of the system, i.e., parallel to the shaft axis. The z- and y-axes of both point in radial directions, i.e., perpendicular to the axis of the shaft. All accelerometer channels were active and connected to the data acquisition system; however, due to the high sampling rate (100 KS/s/channel), only four channels could be collected. All channels of the first accelerometer were collected, and the x direction channel of the second accelerometer was selected for collection because it had a higher amplitude return than the y and z directions.

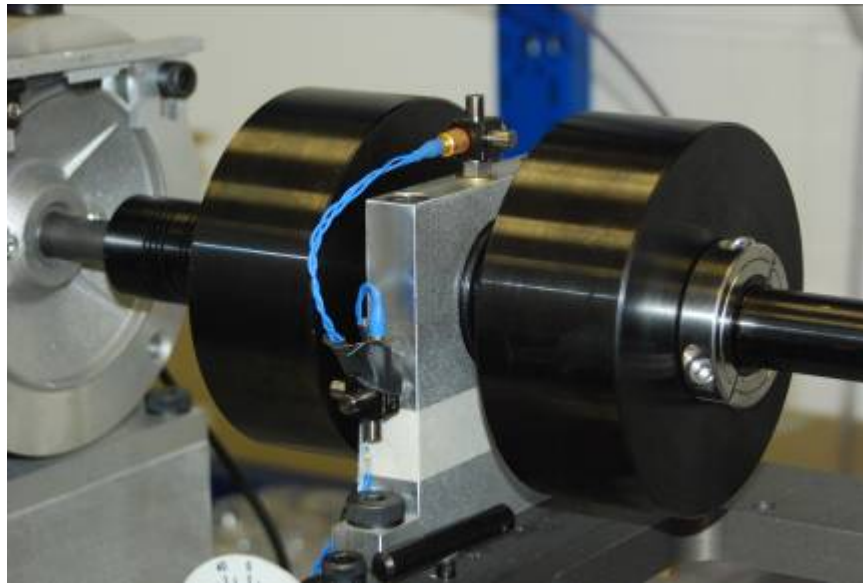


Figure 3. Mounting locations and orientation of the accelerometers.

## II. Revolution Counter (Tachometer)

The test rig was instrumented, from the supplier, with a pulse counter to accurately measure rotational velocity of the drive shaft. The pulse signal from the device/circuitry was recorded as part of the testing for later use in data processing (instantaneous rotational velocity and for techniques requiring time synchronization)

## 2.4 Data Acquisition and Data Recording

### I. Hardware

The data acquisition hardware employed cabling, signal conditioning modules, a data acquisition controller/recorder, and a laptop computer with external hard drive. Figure 4 shows a block diagram of the arrangement of the hardware. Specific components were the following:

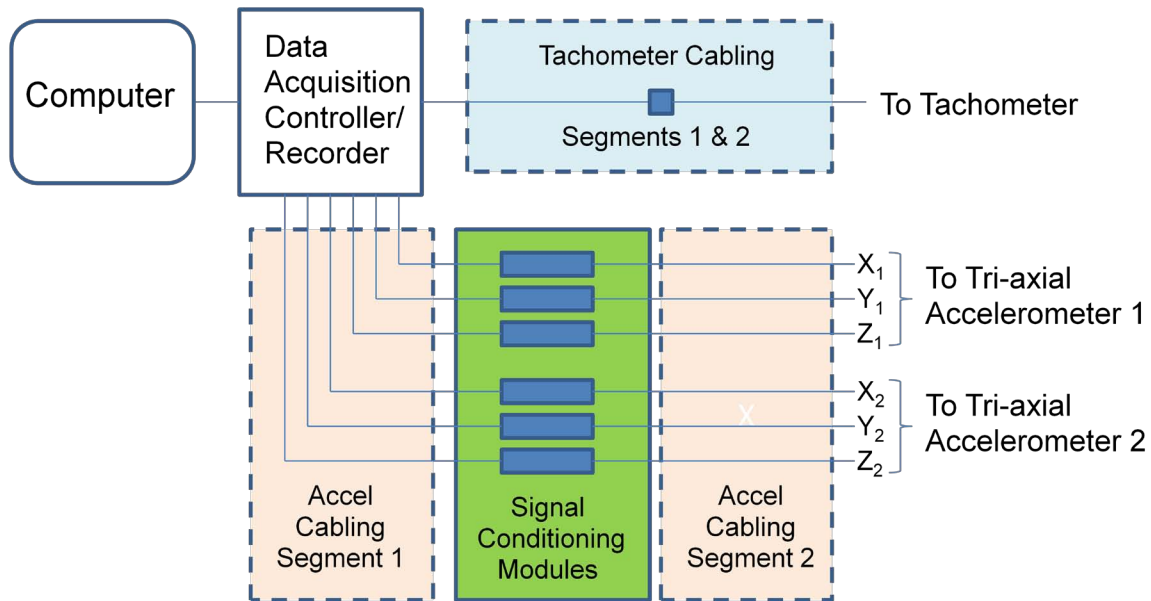


Figure 4. Block diagram of data acquisition hardware.

#### 1. Data Acquisition Controller/Recorder

The system used to acquire the data was the HBM SoMat eDAQ-lite, as shown in figure 5 (appendix A-3). It is modular, composed of “layers:” a mandatory base layer housing the power supply, the processor and storage media (ELCPU), and a variable number of stacked input and output layers, which provide power to sensors, perform analog to digital conversion, and pass the incoming data to storage on the base layer. In our case, there was the base layer plus seven “high level layers” (ELHLS) and a digital input/output (I/O) layer. However, only two of the ELHLS were used in this series of tests. None of the digital I/O channels were used. Each ELHLS layer has four channels of simultaneously sampled differential analog inputs. Of these eight available channels, inputs were provided to only seven; and of these, five were selected for actual data collection. Each of the five channels was simultaneously sampled at 100 KS/s. The base layer interfaces with a PC via a RJ45 Ethernet connection for configuring and initiating a data collection run as well as retrieving data temporarily stored on the base layer.



Figure 5. eDAQ-lite data acquisition controller.

## 2. Signal Conditioning Modules

HBM SoMat ICP type signal conditioning modules (ICP-B-2) were employed on each channel of the accelerometers (appendix A-4). The module provides both power to the accelerometer circuitry and removes the bias on the returning vibration signal. The modules were installed in-line between the accelerometer's connectors and channel inputs on the eDAQ-lite. Since there were two accelerometers and each accelerometer has three channels, there were total of six modules. However, as mentioned previously, only four of the channels were selected for data collection.

## 3. Cabling

The system employed cabling for both the accelerometers and the tachometer pulse signal.

### a. Accelerometer Cabling

1. Cabling for each of the accelerometers consisted of two segments (figure 6). The first segment connected an accelerometer on one end to signal conditioning modules on the other ends. Note that since the accelerometers are tri-axial, there are three outputs per accelerometer each requiring a signal conditioning module. The first segment consisted of Vibra-Metrics P/N 9356232, which splits into three coaxial cables each terminating in an adaptor, Vibra-Metrics P/N CN2-0006-0000. Each adaptor, then, connected to a signal conditioning module. The

second segment consisted of a cable, SoMat P/N SAC-EXT-MF-5, and connected each signal conditioning module to a channel on the eDAQ-lite.

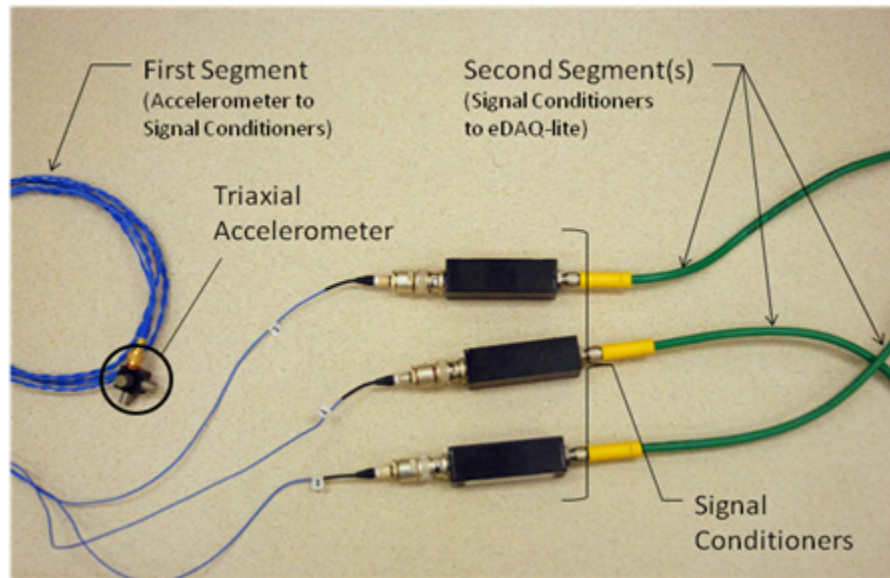


Figure 6. Accelerometer cabling and signal conditioning modules.

#### b. Tachometer Pulse Cabling

To transfer the tachometer signal to the data acquisition system, two segments of cable were required (figure 7). The first was a standard coaxial with a male Bayonet Neill-Concelman (BNC) connector on one end and alligator clips on each of the two leads of the other end. The BNC connector was connected to an existing female connector on the test rig where the pulse is generated; the alligator clips on the opposite end were connected to the second segment. The second segment was a shielded 5-wire/26-AWG cable purchased from HBM SoMat (P/N SAC-TRAN-MP-2). One end of this segment connects to a channel on the data acquisition system. On the other end, as seen in figure 5, the red wire was connected to the positive alligator clip of the first segment, described above, and the green wire was connected to the negative alligator clip; the additional three wires were not used and remained unconnected.

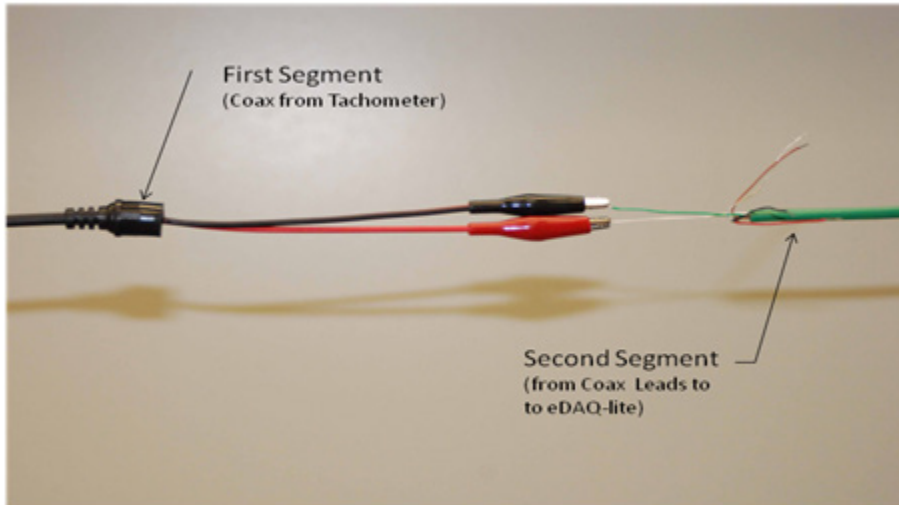


Figure 7. Tachometer cabling focused on transition from coax to eDAQ-lite cabling.

#### 4. Computer

Dell Latitude E6400 Laptop with an Intel Core 2 Duo CPU, P8600 2.4 GHz Processor, 4 GB of RAM, and a Windows Vista 32-bit operating system. The U.S. Army Research Laboratory (ARL) barcode is NB10306.

#### II. Software

Three software programs were employed to collect and analyze the data. HBM's TCE v3.11.0 build 227 was used to program the hardware; check sensor functionality; and collect, record, and download the data. After the data was downloaded onto the laptop, HBM's Infield v2.3.0 was used to review it, specifically by plotting and limited analysis of the data. This was essential to verify sensor functionality and ensure that various aspects of the data collection were being performed as expected. A secondary purpose of Infield was to convert the proprietary binary data into ASCII data. Finally, Mathwork's Matlab R2010b software was used for further analysis of the data. The analysis was a preliminary assessment of trends in the data.

---

### 3. Experimental Procedure

---

#### 3.1 Overview

There were a total of 20 bearings, 5 “good” and 15 with faults described elsewhere. The goal of this effort was to gather sufficient data on the operational performance of the bearings such that data analysis would be meaningful. With this in mind, multiple runs of a predetermined length of time were made for each bearing. Based on previous testing, a 10-s data collection period was determined to be sufficient time for each run, and 10 runs for each bearing was determined to

provide an adequate statistical representation. In addition, two operating conditions were evaluated. The two operating conditions were with (1) the motor driving the weighted shaft only and (2) the pulleys/belts, gearbox, and magnetic load included. The first case is performed to reduce system noise, and the second case is performed to intentionally introduce real-world noise.

### **3.2 Rotational Frequency**

The nominal shaft frequency for all of the runs was selected to be 35 Hz (2100 RPM). This frequency was chosen because it is high enough to commence initial startup (overcome the loads in the system); low enough to keep system audio noise below the safety limit requiring earmuffs; and at a frequency that is not any multiple or division of 60 Hz, the power input frequency. The nominal frequency of 35 Hz could not be set or maintained exactly. The desired frequency was keyed in on a control box, with an adjustment resolution of 0.1 Hz. The actual frequency was monitored in real time on the tachometer display. To achieve the desired frequency, the control box setting was then adjusted until the desired operating frequency was achieved within the resolution of the control. In addition, during the course of a run, the actual frequency tended to drift slightly, more so for the runs with the gearbox and magnetic load connected.

### **3.3 Data Acquisition Software Preparation**

To be ready for data acquisition, the TCE software had to be configured. After opening the software, a “setup” file was constructed. This file controls the entire data collection process including which channels to sample, sample rate, naming of channels, triggers, sensor calibration, power to the sensor, and data storage options. Detailed steps in the construction of a setup file can be found in the eDAQ-lite User’s Manual. What will be presented here are the significant inputs to the file for the performance of these experiments. Wording enclosed in quotes indicates that this is the actual terminology that appears in the software.

- I. All sensors were connected to the eDAQ-lite, the computer and eDAQ-lite system were powered on, and the TCE software was started.
- II. A “New Setup” was created.
- III. In the “Hardware” window by selecting the “Query” button communication with the eDAQ-lite was established, and the window self-populated with the functional elements of the eDAQ-lite.
- IV. In the “Transducer and Message Channel” window, details of channels were defined for each of sensors. This was performed for the four accelerometer channels, all of which had identical inputs except the channel name, and for the tachometer channel.
  1. The accelerometer channels were selected to be “High Level SS” types and “ICP Accelerometer[sensitivity:100mv/g]” was selected for each which provides default values. By selecting them as ICP Accelerometers, the program automatically defines

that a constant current at 24 V will be supplied to the devices. In the two windows that then appear for a “High Level SS Channel,” the physical channels for each accelerometer were selected and named: “Units” were set to “g’s,” the “Output Sample Rate” was set to 100000 Samples/second, the “Output Data Type” was set to “32-bit Float,” the “Full Scale” was set to a “Min” of –150g’s and to a “Max” of 150g’s. In addition, the accelerometers were calibrated such that with a “Defined Value” of 0g’s the “Input Signal” would be 0 V and at a “Defined Span” of 1g the “Input Signal” would be 0.01 V, which describes a sensitivity of 10 mv/g with no offset.

2. The tachometer channel was selected to be a “High Level SS” type and “Voltage Input[10000mv range]” was selected to provide default values. In the two windows that then appear for a “High Level SS Channel,” the physical channels for the tachometer was selected and named: “Units” were set to “Volts,” the “Output Sample Rate” was set to 100000 Samples/second, the “Output Data Type” was set to “32-bit Float,” the “Full Scale” was set to a “Min” of –10 V and a “Max” of 10 V. In addition, the tachometer was calibrated such that with a “Defined Value” of 0 V the “Input Signal” would be 0 V and at a “Defined Span” of 1 V the “Input Signal” would be 1 V, which is 1 to 1 scaling with no offset.
- V. In the “Data Mode Setup,” window parameters were defined for recording of the data. All five transducer channels identified above were selected for recording. The “Triggering Option” was selected to be “Always On.” The “Floats→Data Type” entry was selected to be “FLT32→FLT32,” which caused the data to be saved as 32-bit floating-point numbers. The “Data Storage” was selected to be “PC Card, DRAM, Internal Flash.” Note that this process defines storage into the memory of the eDAQ-lite; permanent storage is later accomplished by uploading the data onto the computer.
- VI. The setup file was saved with the filename 100KHz rate 2xls\_pulse\_x2 only.tce. This setup file was used for all of the runs on bearings with defects.
- VII. The above setup file was copied and the name Good Bearing Only.tce was given to the new setup file. The Good Bearing Only.tce file was altered so that the range of the accelerometers would be lower; specifically, the “Full Scale” was set to a “Min” of –10g’s and a “Max” of 10g’s. By reducing the range the resolution was increased. The Good Bearing Only.tce file was used for data collection on all good bearing runs.

### **3.4 Procedure**

The following test procedure applied for each bearing under test. The procedure was duplicated for each bearing, once with the shaft operating freely and once with the gearbox and magnetic load connected using the belts and the pulleys.

- I. Prepare rig and bearing under test

1. The test rig was disconnected from the main power supply.
2. The socket head screws on the bearing mounts were loosened and the upper half of the mounts was removed. Care must be taken with the bearing under test mounting block to assure that the accelerometer is not damaged and that the accelerometer cables are not disturbed.
3. The two socket head screws on the shaft coupling were loosened and the coupling slid toward the motor until the end of the primary shaft was clearly visible.
4. The entire shaft (with weights and bearings) was removed and placed in a working area.
5. The four socket head screws that secure the motor-end weight to the shaft were loosened and the weight was removed from the shaft.
6. The two set screws that secure the bearing under test to the primary shaft were loosened and the bearing present (previous bearing under test) was removed.
7. The previous bearing was replaced with the current bearing under test. The bearing was precisely located on the shaft by sliding it onto the shaft until it came in contact with the weight that was still on the shaft. The two set screws that secure the bearing to the shaft were then tightened. For “Outer Race Fault” bearings only, the bearing was oriented such that the marking on the bearing (which indicates fault location) was down, i.e., in the lowest possible position.
8. The motor-end weight was placed back on the shaft and located so that left collar of the weight was flush with the step in the shaft. The weight was secured in place by tightening the socket head screws on the collars.
9. The shaft assembly was put back in place on the rig such that the bearings seated properly in the bearing mounts. Each time this procedure was performed, verification was made that there was a gap between the motor end weight and bearing under test mounting block to avoid rubbing.
10. The upper halves of the mounting blocks were returned to their respective locations and the socket head screws tightened to a torque of 15 ft-lbs. Note: Previous testing indicated that the torque on these screws may affect the accelerometer signals.
11. The shaft coupling was repositioned and its two set screws tightened.
12. The cover of the rig was closed and latched.
13. The main power was connected to the test rig.

14. Correct operation of the machinery was made prior to a formal run. This was performed by depressing the green “run” button on the test rig control panel and shortly thereafter depressing the red “stop” button (figure 8). If anything was noted as not performing properly, corrective action was taken.



Figure 8. Test rig control panel.

- II. Using the control panel (figure 8), the operating frequency was set to 35 Hz. Operation of the machine was begun by depressing the “run” button on the control panel.
- III. Using the frequency control buttons on the control panel (the up and down arrows), the frequency was adjusted as necessary to achieve a tachometer reading of as close to 35 Hz as possible. For weights and shaft only runs, the typical control setting was 35.4 Hz. For runs with the gearbox and load connected, the typical control setting was 36.4 Hz.
- IV. The system was allowed to run for 5 min, and the frequency was adjusted again if necessary.
- V. Data collection
1. With the TCE software running and the appropriate initiation of the software as described in section 3.3, the “run” button on the “TCE Test Control Panel” window was selected (figure 9).

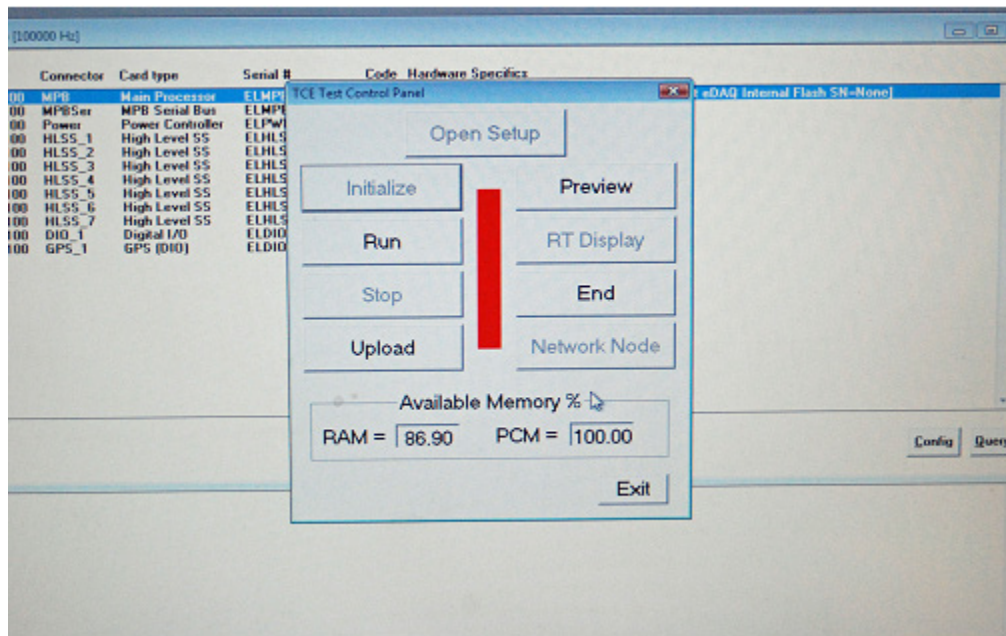


Figure 9. TCE software test control panel.

2. A window appeared, which had a “start run” button, as well as an option to enter a description of the run; the “start run” button was then selected.
  3. The “run time” clock, which appeared on the “TCE Test Control Panel” window, was monitored and the “stop” button was selected when the run time had reached 10 s.
  4. The software was then ready for another run of the same bearing.
  5. The machine was allowed to run without data collection for 1 min.
  6. Steps 1 through 5 were then repeated nine times for a total of 10 runs.
  7. The data was then uploaded to the computer for the 10 runs by selecting the “upload” button on the TCE Test Control Panel and supplying an appropriate filename for the set of runs, e.g., “Ball Fault Level 5”.
  8. The “END” button on the TCE Test Control Panel was then selected. Note: This completed the data collection of a specific bearing under test for the condition of a bearing without connection to the gearbox and magnetic load.
- VI. For the same bearing used in data collection in the previous subsection V, data was collected with the gearbox and magnetic load connected.
1. The two belts were installed onto the pulleys of the primary shaft and gearbox shaft.
  2. Procedures II through V-8 were repeated. Note: The data collection of a particular bearing was then finished.

VII. A new bearing to be tested was selected and procedures I through VI were repeated. The procedure was repeated until data on all bearings was collected.

## 4. Data Storage and Data Conversion

The following are the procedures for data storage and data conversion:

- I. When the data was uploaded to the computer in the procedure in section 3, it was done so with descriptive names and stored in a systematic folder structure. The data, as uploaded, was in a proprietary binary format and is identifiable by “.sie” as the file extension. Tables 1 and 2 show the file structure naming of these files.

Table 1. File naming and folder structure for uploaded files (no gears or load).

Folder	1 in Bearing Fault Tests			
Folders	No Load			
Folders	Good Bearing	Ball Fault	Inner Race Fault	Outer Race Fault
File names	Good Bearing1.sie	Ball Level 1.sie	BIR Level 1.sie <sup>a</sup>	BOR Level 1.sie <sup>b</sup>
	Good Bearing2.sie	Ball Level 2.sie	BIR Level 2.sie	BOR Level 2.sie
	Good Bearing3.sie	Ball Level 3.sie	BIR Level 3.sie	BOR Level 3.sie
	Good Bearing4.sie	Ball Level 4.sie	BIR Level 4.sie	BOR Level 4.sie
	Good Bearing5.sie	Ball Level 5.sie	BIR Level 5.sie	BOR Level 5.sie

<sup>a</sup> BIR is an abbreviation of Bearing Inner Race

<sup>b</sup> BOR is an abbreviation of Bearing Outer Race

Table 2. File naming and folder structure for uploaded files (with gears and load).

Folder	1 in Bearing Fault Tests			
Folders	Loaded			
Folders	Good Bearing_P	Ball Fault_P	Inner Race Fault_P	Outer Race Fault_P
File names	Good Bearing1_P.sie	Ball Level 1_P.sie	BIR Level 1.sie	BOR Level 1.sie
	Good Bearing2_P.sie	Ball Level 1_P.sie	BIR Level 2.sie	BOR Level 2.sie
	Good Bearing3_P.sie	Ball Level 1_P.sie	BIR Level 3.sie	BOR Level 3.sie
	Good Bearing4_P.sie	Ball Level 1_P.sie	BIR Level 4.sie	BOR Level 4.sie
	Good Bearing5_P.sie	Ball Level 1_P.sie	BIR Level 5.sie	BOR Level 5.sie

- II. To analyze the data, it was converted from binary into ASCII format. Specifically, all accelerometer data for a particular run was written in ASCII text format as four tab delimited columns into an appropriately named file. This was repeated for each run, totaling 400 files. The tachometer data was not converted at this time. The data conversion was performed by first reading a “.sie” file into the Infield software, selecting the desired data, overplotting it as a function of time, and saving the plotted data as an ASCII File.
- III. Clear organization of the ASCII data was deemed critical for ease of identification and access in later use. Table 3 shows a portion of the file structuring and naming. For the remaining files and folders, the same format is followed with 10 ASCII files for each fault level of each fault type for both “No Load” and “Load.” The additional naming followed a descriptive convention and can be briefly described as follows:
- Under the No Load folder the subfolders were Good Bearings, Ball Faults, Inner Race Faults, and Outer Race Faults.
  - Under each of these folders were subfolders with the names Good Bearing 1-5, Ball Fault Level 1-5, Inner Race Fault Level 1-5, and Outer Race Fault Level 1-5.
  - Under each of these folders were the 10 ASCII files with descriptive names, which include the run number, i.e., run1-run10.

The same names were used for the Load folders and files; however, each was followed by “\_P”.

Table 3. Portion of ASCII data showing folders structure and filenames.

Folder	1 in Bearing Fault Tests			
Folder	ACII Data			
Folders	No Load			
Folders	Good Bearings			
Folders	Good Bearing 1	Good Bearing 2	Good Bearing 3	Good Bearing 4
File names	Good Bearing 1 _ run1.asc	Good Bearing 2 _ run1.asc	Good Bearing 1 _ run1.asc	Good Bearing 1 _ run1.asc
	Good Bearing 1 _ run2.asc	Good Bearing 2 _ run2.asc	Good Bearing 1 _ run2.asc	Good Bearing 1 _ run2.asc
	Good Bearing 1 _ run3.asc	Good Bearing 2 _ run3.asc	Good Bearing 1 _ run3.asc	Good Bearing 1 _ run3.asc
	Good Bearing 1 _ run4.asc	Good Bearing 2 _ run4.asc	Good Bearing 1 _ run4.asc	Good Bearing 1 _ run4.asc
	Good Bearing 1 _ run5.asc	Good Bearing 2 _ run5.asc	Good Bearing 1 _ run5.asc	Good Bearing 1 _ run5.asc
	Good Bearing 1 _ run6.asc	Good Bearing 2 _ run6.asc	Good Bearing 1 _ run6.asc	Good Bearing 1 _ run6.asc
	Good Bearing 1 _ run7.asc	Good Bearing 2 _ run7.asc	Good Bearing 1 _ run7.asc	Good Bearing 1 _ run7.asc
	Good Bearing 1 _ run8.asc	Good Bearing 2 _ run8.asc	Good Bearing 1 _ run8.asc	Good Bearing 1 _ run8.asc
	Good Bearing 1 _ run9.asc	Good Bearing 2 _ run9.asc	Good Bearing 1 _ run9.asc	Good Bearing 1 _ run9.asc
	Good Bearing 1 _ run10.asc	Good Bearing 2 _ run10.asc	Good Bearing 1 _ run10.asc	Good Bearing 1 _ run10.asc

---

## 5. Preliminary Data Analysis and Results

---

As indicated earlier the primary goal of this effort was to collect data on faulted bearings, which could be used to develop algorithms for health monitoring and predict remaining life. With this in mind, it was deemed prudent to make a cursory examination of the data to determine whether features could be extracted from it that follow trends with damage type and level.

- I. A limited but representative display of raw time series data is presented in figures 10, 11, 12, and 13. Time series data for a Good Bearing and Level 1 and Level 5 of each fault type from the z-axis of the top accelerometer are shown. Note that the difference between the two levels are easily discernable, giving a good indication that they should be distinguishable computationally. The scales are constant only for the two levels of each fault type. The scale of the Good Bearing run was selected as the lowest range in the other plots, which is Ball Fault Level 5,  $\pm 20g$ 's.

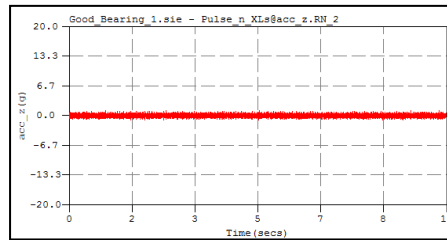


Figure 10. Raw time series data for a good bearing.

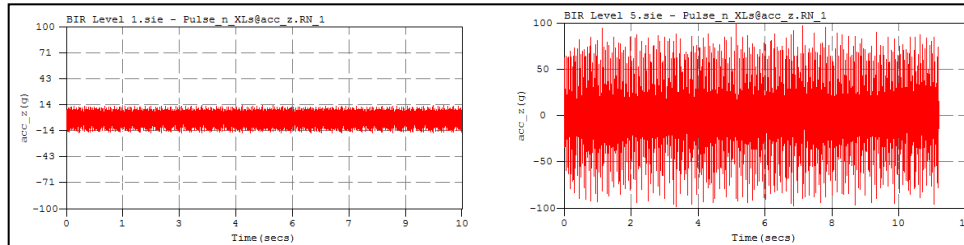


Figure 11. (Left) Inner race fault level 1 data and (right) inner race fault level 5 data.

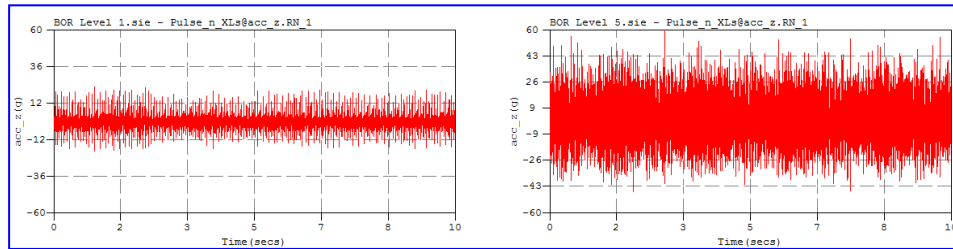


Figure 12. (Left) Outer race fault level 1 data and (right) outer race fault level 5 data.

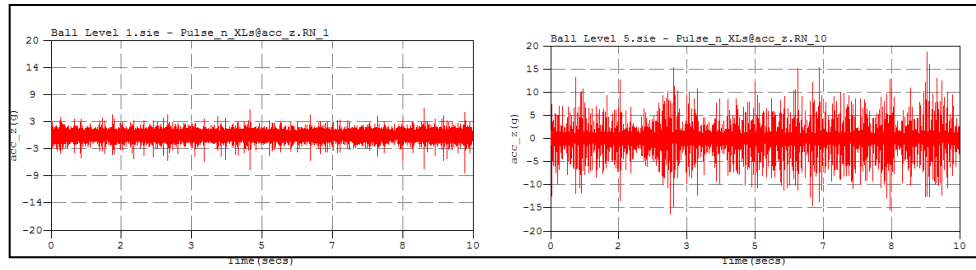


Figure 13. (Left) Ball fault level 1 data and (right) ball fault level 5 data.

II. Statistical features, including root mean square (RMS), Kurtosis, Skewness, Crest Factor, and Peak to Peak, were examined, on a limited basis, to see if trends existed. In general, RMS and Peak to Peak show increasing trends with fault level for all fault types, as seen in figures 14 and 15. A few data points are present that do not follow a monotonic trend and will require further investigation. The other statistical features appear less suited for bearing fault level analysis, that is, clear trends are not apparent at this point. It bears repeating that the calculations were performed on a limited amount of the data, one run per fault for each fault level, and that analysis of the complete data set will be necessary to be more conclusive.

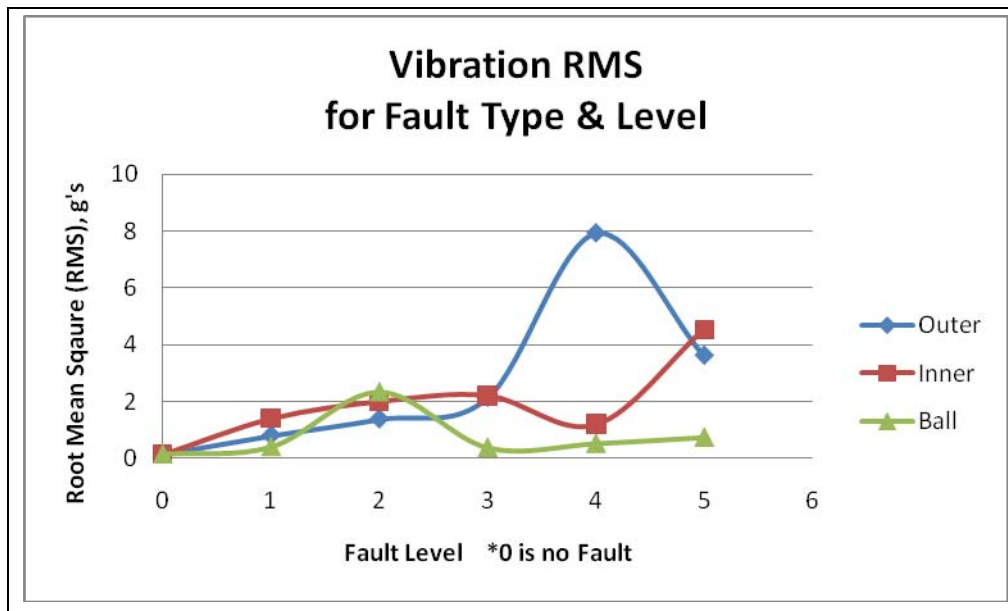


Figure 14. Vibration RMS as a function of fault level and fault type.

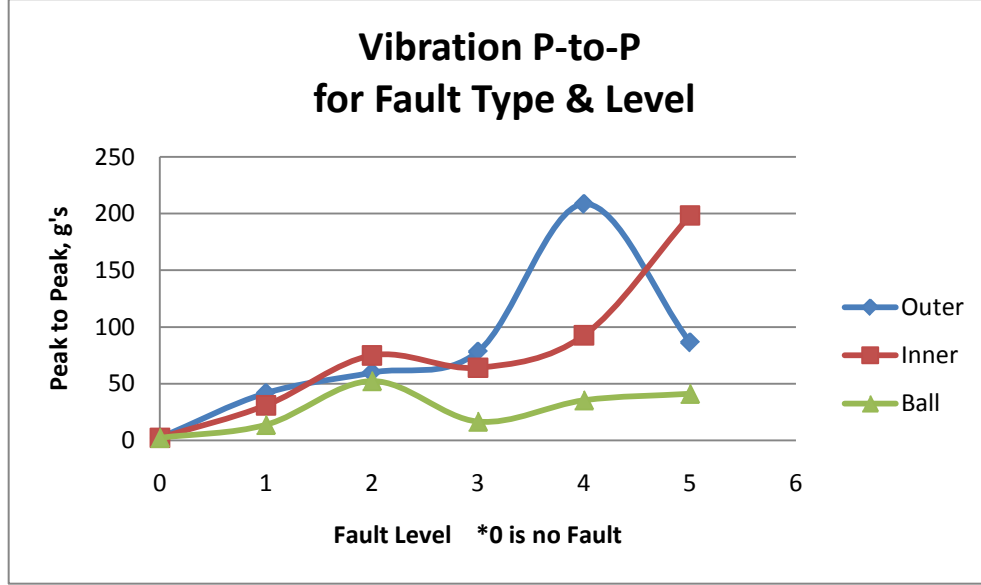


Figure 15. Vibration peak to peak values as a function of fault type and fault level.

III. An examination of the characteristic frequencies associated with bearing geometry, also known as bearing defect frequencies, was performed. The presence and amplitude of the defect frequencies were expected to be indicators of the detectability and classification of the particular fault and level of damage. For this examination, what is commonly known as envelope analysis was performed. This was accomplished by taking the fast Fourier transform of the magnitude of the Hilbert transform of the raw data, plotting it in the frequency domain, and looking for the presence and magnitude of the defect frequencies.

1. The formulae for the defect frequencies are:

$$BPFI = \frac{n}{2} \left( 1 + \frac{BD}{PD} \cos \theta \right) * f \quad (1)$$

$$BPFO = \frac{n}{2} \left( 1 - \frac{BD}{PD} \cos \theta \right) * f \quad (2)$$

$$FTF = \frac{1}{2} \left( 1 - \frac{BD}{PD} \cos \theta \right) * f \quad (3)$$

$$Rolle = \frac{PD}{BD} \left( 1 - (BD/PD)^2 \cos^2 \theta \right) * f \quad (4)$$

$$BSF = \frac{PD}{2BD} \left( 1 - (BD/PD)^2 \cos^2 \theta \right) * f \quad (5)$$

where

Ball pass frequency inner (BPFI) = the frequency corresponding to a defect on the inner race

Ball pass frequency of the outer race (BPFO) = the ball pass frequency of the outer race and corresponds to a defect on the outer race

FTF = the fundamental train frequency

BSF = the ball spin frequency

Rolle = the ball defect frequency (roller element)

n = number of balls

BD = ball diameter

PD = pitch diameter

$\theta$  = contact angle

For these experiments, the following is true:

$$n = 9$$

$$BD = 0.3125 \text{ in}$$

$$PD = 1.5157 \text{ in}, \theta = 0$$

$$f = 35 \text{ Hz}$$

The calculated values of the defect frequencies are listed in table 4.

Table 4. Defect frequencies for these experiments.

<b>BPFI</b>	<b>BPFO</b>	<b>FTF</b>	<b>BSF</b>	<b>Rolle</b>
190 Hz	125 Hz	13.9 Hz	81.3 Hz	162.5 Hz

IV. Figures 16 and 17 show results of inner race faulted bearings and a good bearing. The plots focus on a band around the inner race fault frequency of 190 Hz. One can see that the fault frequency is clearly visible (detectable) and that the amplitude grows with fault level. The vertical scale of the good bearing (figure 16, left) is much smaller than figure 16 (right) and figure 17, and any frequency which is in the vicinity of the fault frequency is much lower than that of the faulted bearings.

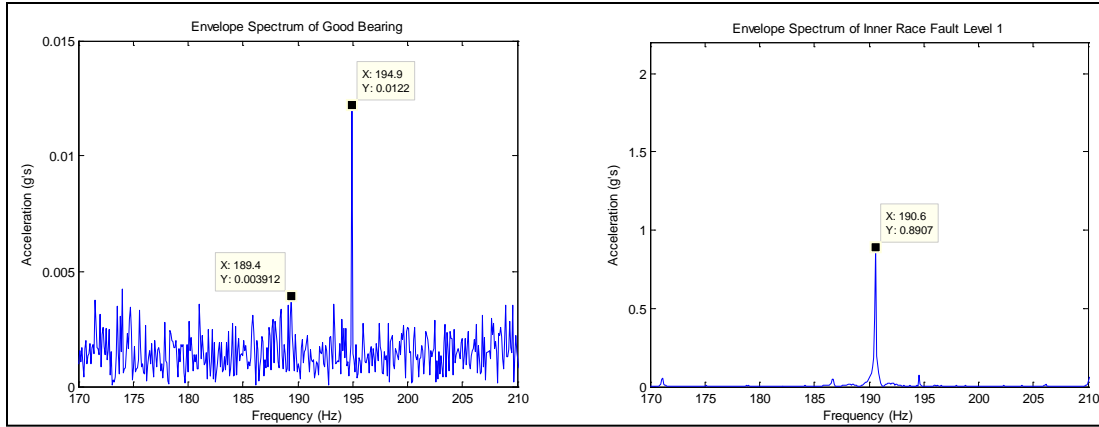


Figure 16. (Left) Good bearing envelope spectrum around BPFI and (right) fault level 1, envelope spectrum around BPFI.

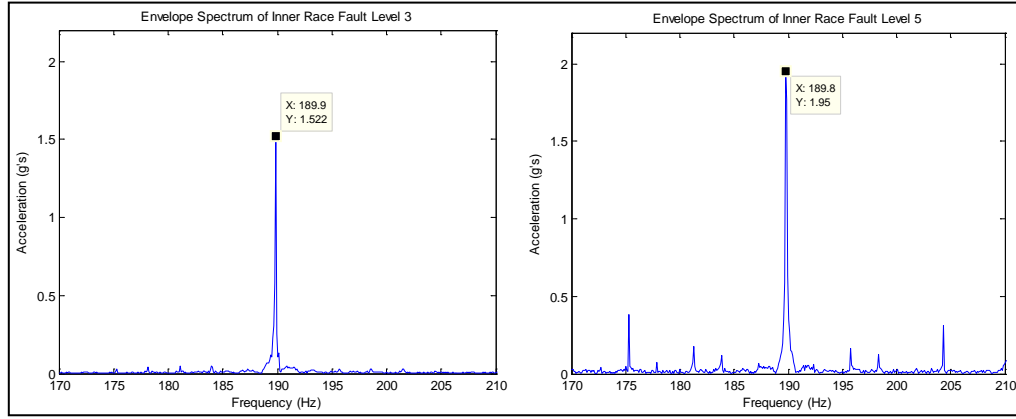


Figure 17. (Left) Fault level 3, envelope spectrum around BPFI and (right) fault level 5, envelope spectrum around BPFI.

V. Figures 18 and 19 show results of outer race faulted bearings and a good bearing. The plots focus on a band around the outer race fault frequency of 125 Hz. Again, the fault frequency is clearly visible, as well as increases with fault level. As with the previous figures, the vertical scale of the good bearing figure is much lower than that of the other figures, and that the magnitude at fault frequency of the good bearing is far less than that of the faulted bearings.

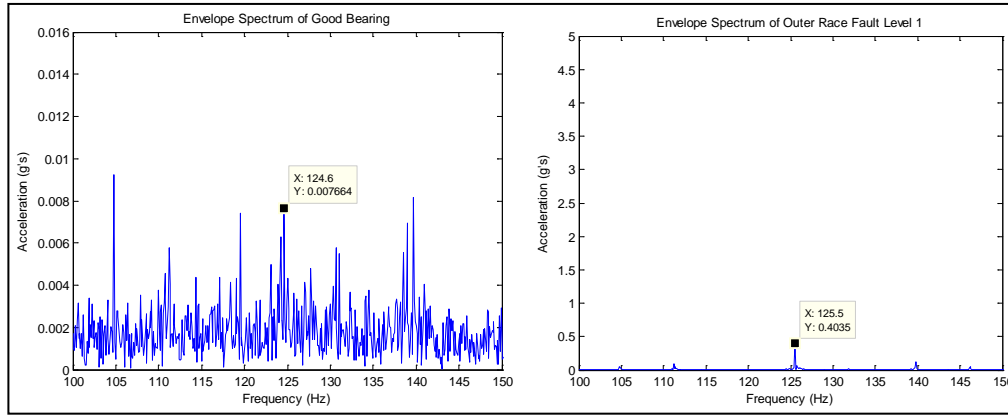


Figure 18. (Left) Good bearing. Envelope spectrum around BPFO and (right) fault level 1, envelope spectrum around BPFO.

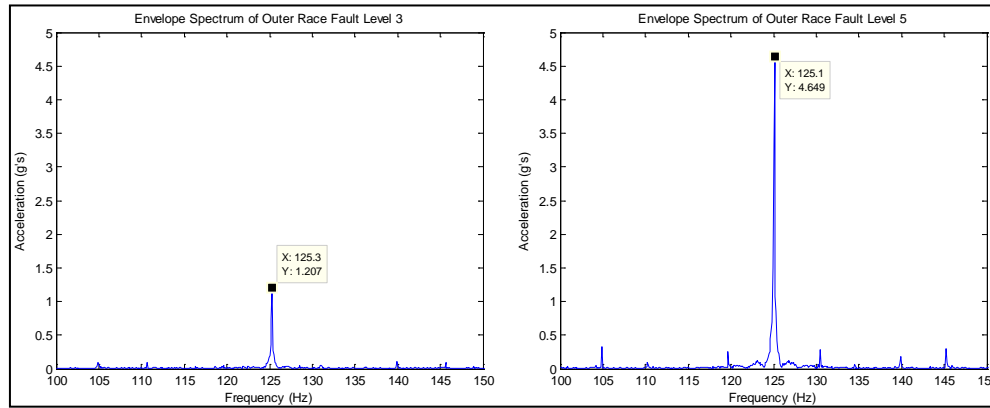


Figure 19. (Left) Fault level 3, envelope spectrum around BPFO and (right) fault level 5, envelope spectrum around BPFO.

- i. Figures 20 and 21 show the results of the ball faulted bearings and a good bearing. In this case, the low end of the spectrum was examined, because it was noted that the fundamental train frequency and its harmonics are clearly visible and increase with the fault level. A plot of the good bearing data was not included, because the fundamental train frequency, or harmonics, could not be distinguished from the noise; even identification at fault level 1 is questionable. As an additional note, there were several low level peaks in the vicinity of the roller element defect frequency that were not present in the good bearing spectrum. Further analysis is necessary and is hoped to reveal that this portion of the spectrum will provide beneficial information (features), as well.

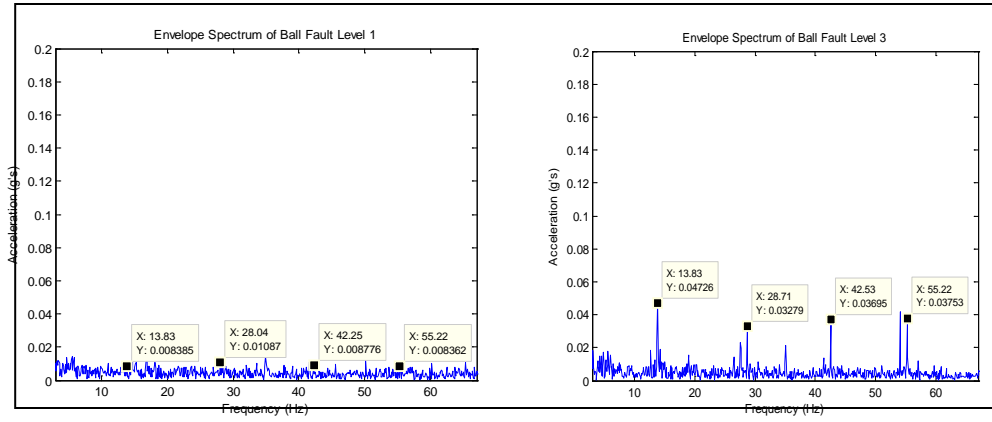


Figure 20. (Left) Ball fault level 1. Low end of envelope spectrum and (right) ball fault level 3, low end of envelope spectrum

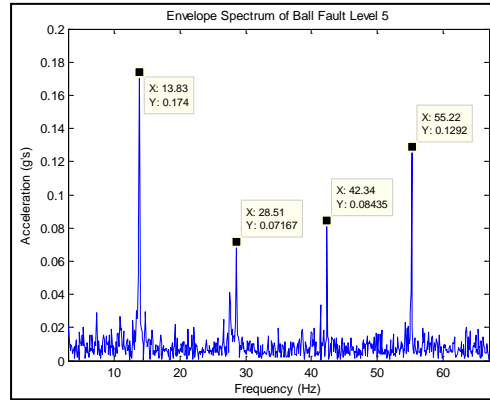


Figure 21. Ball fault level 5, low end of envelope spectrum.

## 6. Summary and Conclusions

A substantial amount of data was collected on ball bearings with known levels of seeded faults, as well as healthy bearings. Based on initial examination of the data, it seems clear that a number of features exist, even beyond those that were examined, which can be exploited in the detection and classification of specific faults in the bearings. A great deal of work still remains to be done on the analysis of the data. This includes processing and correlating all the data for features already mentioned, as well as employing additional signal processing methods, which are likely to include wavelet analysis, time-frequency analysis, statistical features of transformed data, and the application of neural nets. All in all, with the appropriate application of data processing techniques, it is expected that this work will be uniquely beneficial for P&D purposes since it includes both ground truth and discrete fault levels and types.

---

## Appendix. Bearing and Test Equipment Specifications

---

The following is a short description of the hardware and sensors used during this data collection.

### A-1 ER16K Ball Bearing, Manufactured by Rexnord Industries, LLC

Figure A-1 shows the ER16K bearing used throughout the experiments.



Figure A-1. ER16K bearing used throughout the experiments.

#### *Specifications:*

Diameter of the Shaft:	1 in
Diameter - Outside:	2.0472 in
Rolling Element:	Ball
Ability to Relubricate:	Yes
Bore Shape:	Round
Distance from Bearing Centerline to Centerline of Lube Groove:	0.185 in
Distance from Outer Ring Face to Snap Ring Face:	0.09375 in
Duty Type:	Standard Duty (Normal)

Inner Ring Fillet Radius:	0.04 in
Inner Ring Hub Diameter:	1.313 in
Length Through Bore:	1.375 in
Locking Collar Outside Diameter:	1.5625 in
Locking Collar Type:	Centrik-Lok Locking Device
Locking Collar Width:	0.34375 in
Outer Ring Width:	0.749 in
Short Hub Length:	0.508 in
Size Code:	205
Snap Ring Outside Diameter:	2.265625 in
Snap Ring Width:	0.046875 in
Thread Size:	1/4-28
Type of Seal:	Single Lip Seal

## **A-2 Machine Fault Simulator, Manufactured by SpectraQuest, Inc.**

Figure A-2 shows the machine fault simulator.



Figure A-2. Machine fault simulator.

### *Specifications:*

#### **Electrical:**

Voltage:	115/230 VAC, Single phase, 60/50 Hz
Motor:	3 Phase, 1 HP, pre-wired self-aligning mounting system
Drive:	1 HP variable frequency AC drive with multi-featured front panel programmable controller
RPM Range:	0 to 6000 rpm (short duration) variable speed
Tachometer	Built-in tachometer with liquid crystal display (LCD) display and one pulse per revolution analog transistor-transistor logic (TTL) output for DAQ purposes

#### **Mechanical:**

Shaft Diameter	1 in diameter; turned, ground, and polished (TGP) steel
Bearing	Two sealed rolling element in aluminum horizontally split bracket housing for easy changes, tapped for transducer mount. Bearing mounts can be mounted in five different positions for variable rotor span.
Rotor Base	18 in long, completely movable using jack bolts for easy horizontal misalignment and standard shims for vertical misalignment. Pinned for easy realignment.
Belt Mechanism	Two double groove “V” belt with one set screw mounting and one bush/key mounting. Positive displacement lever with turnbuckle plus adjustable gearbox platform.
Gearbox and Brake	Accessible three-way straight cut bevel gearbox with 1.5:1 ratio (20 gear input). Manually adjustable magnetic brake 0.5–10 lb-in

#### **Instrumentation:**

Connectors	16 Bayonet Neill-Concelman (BNC) connector plate under the rotor base linked to BNC connector panel mounted on the edge for the base plate for direct connection to data collectors.
Safety Cover	Lockable clear, impact resistant hinged plastic cover with motor interlock switch to shut down motor when cover is raised.
Foundation	½-in die-cast aluminum base, base stiffener, and eight rubber isolators

**Physical:**

Weight	Approximately 130 lb
Dimensions	L=39 in (100 cm), W=25 in (63 cm), H=21 in (53 cm)

**A-3. SoMat eDAQ-lite by HBM, Inc.**

The SoMat eDAQ lite (figure A-3) is a standalone data acquisition system. It performs signal conditioning and a capacity to perform onboard data processing. The eDAQ-lite is modular, consisting of a required base layer, *ELCPU*, and for this experiment seven layers of four simultaneously sampled high-level differential analog inputs, *ELHLS* layers, and, although not used in this experiment, a digital input/output layer (*ELDIO*).



Figure A-3. SoMat eDAQ-lite.

*Specifications:***Physical:**

Size:	6.875 in wide x 5.625 in long x 7.75 in high
Temperature:	–20 to 65 °C
Connectors:	6-pin M8

**Enclosure:**

Sealed System:	Machined aluminum case and sealed gaskets protect the system from humidity, corrosion, water spray, and dust.
Vibration Tested:	Swept sine tested from 5 to 2000 Hz at 20g's
Modular:	Up to eight layers can be custom configured pending testing requirements. The removal of four screws is all that is required to disassemble a system.

**System:**

Input Power: ELCPU: 10–18 VDC  
Fuses: 10 A, automotive mini-blade  
Internal Back-up Battery

**Sample Rates:**

Master Clock Rates: 100 kHz = 0.1 Hz to 100 kHz  
98.3 kHz = 0.1 Hz to 98,304 Hz

**Communications:**

Ethernet: 100 BaseT  
Serial: RS232 up to 115,200 baud

**Memory:**

Internal Flash: 2 GB  
Internal DRAM: 64 MB

**A-4. SoMat ICP-Type Signal Conditioning Module (ICP-B-2) by HBM, Inc.**

This module (figure A-4) supplies a regulated 4-mA current source to an integral electronics piezoelectric (IEPE) transducer. Constant current biased transducers require AC coupling for the output signal. The ICP-Type Signal Conditioning Module uses a 1 microfarad–1 M $\Omega$  coupling network which forms a 0.159-Hz high pass input filter. That is, a sinusoidal input signal at 0.159 Hz will be attenuated by 3 db, (output signal at 70.7% of input). Frequencies below 0.159 Hz will be attenuated more, higher frequencies less.



Figure A-4. SoMat ICP-B-2.

*Specifications:*

**Physical:**

Size:	0.75 in wide x 3.25 in long x .75 in high (1.905 cm W x 8.255 cm L x 1.905 cm H)
Weight:	0.08 lbs (0.03 kg)
Temperature:	–20 to 65 °C
Connectors:	SoMat 6-Pin M8, BNC or 10-32 Coax

**Inputs:**

Input Power:	24 VDC at 4 mA
Load:	1 M $\Omega$

**A-5 Vibra-Metrics Model 3000 Tri-axial Accelerometer**

Figure A-5 shows the Vibra-Metrics model 3000.



Figure A-5. Vibra-Metrics model 3000.

*Specifications:*

Sensitivity:	at 100 Hz, $\pm 5\%$ 10 mV/g, 1.02 mV/(m/s <sup>2</sup> )
Frequency Range:	<ul style="list-style-type: none"><li>• <math>\pm 5\%</math> 3 Hz, 7 kHz</li><li>• <math>\pm 10\%</math> 2 Hz, 8 kHz</li><li>• <math>\pm 3</math> dB 1 Hz, 10 kHz</li></ul>
Turn-on Time:	(2% of final bias) <5 s
Amplitude Range:	(at 72 °F) $\pm 500$ g
Mounted Resonance:	>25 kHz

Transverse Sensitivity: <5%

**Electrical:**

Noise (typical):

- Broadband 2.5 Hz to 25 kHz 1500  $\mu\text{g}$  (rms)
- Spectral 10 Hz 100  $\mu\text{g}/\sqrt{\text{Hz}}$
- 100 Hz 25  $\mu\text{g}/\sqrt{\text{Hz}}$
- 1000 Hz 10  $\mu\text{g}/\sqrt{\text{Hz}}$

Output Impedance: 1000  $\Omega$

Isolation: >100 Meg  $\Omega$

Noise Rejection: (EMI/RFI) >52 dB

Bias Volts (nominal): 7 VDC

Power Requirements: 15–30 VDC

Current Regulating

Diode: 1–6 mA

**Environmental:**

Temperature Range: –40 to 250 °F / –40 to 121 °C

Base Strain: <0.005 g peak/ $\mu\text{strain}$

Shock Limit: 5000 g

**Physical:**

Physical Dimensions:

- .8 in high x .8 in wide x 1.05 in diameter
- 2 cm x 2 cm x 2.7 cm

Weight: 0.35 oz/10 g

Case Material: Titanium

Mounting: 10-32 removable stud

Mounting Torque: 20 in-lb (2.2 N-m)

Connector: Side 4-pin

---

## List of Symbols, Abbreviations, and Acronyms

---

ARL	U.S. Army Research Laboratory
BNC	Bayonet Neill-Concelman
BPFI	ball pass frequency inner
BPFO	ball pass frequency of the outer race
I/O	input/output
IEPE	integral electronics piezoelectric
LCD	liquid crystal display
P&D	Prognostics and Diagnostics
RMS	root mean squared
TGP	turned, ground, and polished
TTL	transistor-transistor logic

NO. OF COPIES	ORGANIZATION
1 ELECT	ADMNSTR DEFNS TECHL INFO CTR ATTN DTIC OCP 8725 JOHN J KINGMAN RD STE 0944 FT BELVOIR VA 22060-6218
1 CD	OFC OF THE SECY OF DEFNS ATTN ODDRE (R&AT) THE PENTAGON WASHINGTON DC 20301-3080
1	US ARMY INFO SYS ENGRG CMND ATTN AMSEL IE TD F JENIA FT HUACHUCA AZ 85613-5300
6	US ARMY RSRCH LAB ATTN RDRL CIO MT TECHL PUB ATTN RDRL CIO LL TECHL LIB ATTN RDRL SER E A BAYBA ATTN RDRL SER E D WASHINGTON ATTN RDRL SER E K TOM ATTN IMNE ALC HRR MAIL & RECORDS MGMT ADELPHI MD 20783-1197

TOTAL: 9 (1 ELEC, 1 CD, 7 HCS)

INTENTIONALLY LEFT BLANK.